Calbindin D28k targets *myo*-inositol monophosphatase in spines and dendrites of cerebellar Purkinje neurons

Hartmut Schmidt[†‡], Beat Schwaller[§], and Jens Eilers[†]

[†]Carl-Ludwig-Institut für Physiologie, Abteilung Neurophysiologie, Medizinische Fakultät, Universität Leipzig, 04103 Leipzig, Germany; and [§]Division of Histology, Department of Medicine, University of Fribourg, 1705 Fribourg, Switzerland

Edited by Erwin Neher, Max Planck Institute for Biophysical Chemistry, Göttingen, Germany, and approved March 9, 2005 (received for review October 22, 2004)

The Ca^{2+}-binding protein calbindin D28k (CB) is vital for the normal function of the central nervous system but its specific functional role is largely unclear. CB is typically described as a mobile Ca^{2+} buffer that shapes the spatiotemporal extent of cellular Ca^{2+} signals. Recent biochemical data, however, indicate that CB also has characteristics of a Ca^{2+} sensor and activates *myo*-inositol monophosphatase (IMPase), a key enzyme of the inositol-1,4,5-trisphosphate signaling cascade and an assumed target of mood-stabilizing drugs in the treatment of bipolar disorder. Here, we show that CB interacts with IMPase in cerebellar Purkinje neurons, a cell type well known to rely on inositol-1,4,5-trisphosphate-dependent synaptic integration. Quantification of the mobility of dye-labeled CB with two-photon fluorescence recovery after photobleaching revealed that a substantial fraction of CB is immobilized in spines and dendrites, but not in axons. Immobilization occurs over several seconds, is increased by suprathreshold synaptic activity, and can be relieved by a synthetic peptide that resembles the putative CB-binding site of IMPase, indicating that CB binds to immobilized IMPase. Measurements of the apparent diffusion coefficients of CB imply that CB does not interact with cytosolic IMPase or that the latter is present only in minute amounts in the spiny dendrites of Purkinje neurons. Our results suggest that CB acts as an activity-dependent sensor that targets membrane/cytoskeleton-bound IMPase in central neurons.

calcium | inositol-1,4,5-trisphosphate | two-photon microscopy | diffusion | mobility

Calbindin D28k (CB) is a member of the EF-hand family of Ca^{2+}-binding proteins and is expressed in distinct cell types throughout the central nervous system and in nonneuronal tissue (1). Each CB molecule consists of six EF-hand motifs, two of which have probably lost their Ca^{2+} affinity. The Ca^{2+}-binding capabilities of the four remaining EF hands have been characterized in detail (2). CB has been shown to effectively shape postsynaptic Ca^{2+} signals (3–5) and to be relevant for certain forms of short-term synaptic plasticity (6). In view of these properties, CB is usually classified as a potent intracellular Ca^{2+} buffer that differs from related proteins such as calbindin D9k or parvalbumin (PV) mainly in its specific Ca^{2+}-binding kinetics, diffusional mobility, and cell-specific expression.

In recent years, evidence showing that CB may be more than a simple Ca^{2+} buffer has been accumulated by Berggård, Linse, and coworkers (7–9) and Kumar, Cavanagh, and coworkers (10, 11). Their *in vitro* studies indicated that CB undergoes conformational changes upon Ca^{2+} binding (8–10) and that CB interacts with *myo*-inositol monophosphatase (IMPase; ref. 7) and Ran-binding protein M (11). Together with older reports on enzyme regulation (12–15) and membrane/cytoskeleton targeting of CB (16, 17), these data suggest that CB not only acts as a potent Ca^{2+} buffer but also as a Ca^{2+} sensor. So far, however, no *in situ* data on the interaction of CB with one of its targets have been reported.

Among the potential targets of CB, IMPase is especially interesting because of its proposed role in the pathogenesis and treatment of manic-depressive (bipolar) disorder (18). IMPase is a key enzyme in the phosphatidylinositol second messenger pathway in which it is responsible for the final step in the degradation of inositol-1,4,5-trisphosphate (IP_3) to *myo*-D-inositol (19). Two isoforms of IMPase have been identified: IMPase-1 and IMPase-2. Both isoforms have been linked to bipolar disorder: the gene for IMPase-2 is localized in a susceptibility region for this disorder on chromosome 18 (20); IMPase-1 is one of the assumed targets of Li^+ in the treatment of bipolar disorder (21). Li^+ has been proposed to inhibit IMPase (21, 22), an effect that seems to be the mode of action for several mood-stabilizing drugs (23). In view of these findings we tested possible interactions of CB and IMPase *in situ* in cerebellar Purkinje neurons (PNs), a cell type well known to express high levels of CB and to use IP_3-mediated signaling for long-term changes of its synaptic connectivity.

Methods

Preparation and Solutions. Acute cerebellar brain slices were prepared from 21- to 24-day-old mice that were decapitated under isoflurane (Abbott, Wiesbaden, Germany) anesthesia. The vermis was removed and mounted in a chamber filled with cooled (0–2°C) artificial cerebrospinal fluid (ACSF). Parasagittal slices (200 μm thick) were cut by using a vibratome (HR2, Sigmann Elektronik, Huffenhardt, Germany) and kept in ACSF at 35°C for 45 min before they were transferred to the recording chamber. Experiments were performed at 20–22°C.

The artificial cerebrospinal fluid contained 125 mM NaCl, 2.5 mM KCl, 1.25 mM NaH_2PO_4, 26 mM $NaHCO_3$, 1 mM $MgCl_2$, 2 mM $CaCl_2$, and 20 mM glucose, gassed with 95% O_2 and 5% CO_2, pH 7.3. The pipette solution was composed of 150 mM K-gluconate, 10 mM NaCl, 3 mM Mg-ATP, 0.3 mM GTP, and 10 mM Hepes dissolved in purified water (W-3500, as all chemicals, from Sigma). The pH was adjusted to 7.3 with KOH. As indicated, 500 μM of 40-kDa fluorescein dextran (Molecular Probes), 200 μM of dye-labeled CB (CB*), and/or 400 μM of a synthetic peptide were added to the pipette solution. Rat recombinant CB expressed in *Escherichia coli* and purified as described for recombinant calretinin (24) was labeled with Alexa 488 by using a commercial kit (Molecular Probes) as described for PV (25); the final molecular Alexa/CB ratio was between 0.4 and 0.7. Synthetic peptides with acetylated N and amidated C

This paper was submitted directly (Track II) to the PNAS office.

Abbreviations: CB, calbindin D28k; CB*, dye-labeled CB; CF, climbing fiber; FRAP, fluorescence recovery after photobleaching; IMPase, *myo*-inositol monophosphatase; IMP-P, peptide resembling the CB-binding site of IMPase; IP_3, inositol-1,4,5-trisphosphate; PN, Purkinje neuron; PV, parvalbumin.

[‡]To whom correspondence should be addressed. E-mail: hartmut.schmidt@medizin.uni-leipzig.de.

www.pnas.org/cgi/doi/10.1073/pnas.0407855102

termini, either the putative CB-binding domain of IMPase-1, ISSIKEKYPSHS (IMP-P; ref. 7), or a scrambled control peptide, SIKHPSKISEYS, were provided by the Interdisciplinary Center for Clinical Research, Leipzig, Germany or a commercial supplier (AnaSpec, San Jose, CA). Identical results were obtained with peptides from both sources. Before use, the pipette solution was filtered (0.2 μm, Nalge).

Dye Loading and Electrical Recordings. PNs were equilibrated with the dye-containing pipette solution in the whole-cell patch-clamp configuration. Current (up to -300 pA) was injected to keep the membrane potential at -60 to -65 mV by using an Axopatch 200A amplifier, a Digidata 1320A AD/DA converter, and CLAMPEX 8.0 software (Axon Instruments). Patch pipettes were pulled from borosilicate glass (Scientific Products) on a P-87 puller (Sutter Instruments, Novato, CA) to resistances of 4–6 MΩ. To allow rapid equilibration of the cytosol with the pipette solution, the series resistance was kept <25 MΩ for at least 15 min after breaking into the cell.

Fluorescence Recovery After Photobleaching (FRAP) Recordings and Data Analysis. Two-photon FRAP experiments were performed as described (25) with a custom-modified Fluoview 300 laser-scanning microscope (Olympus) equipped with a mode-locked Ti:sapphire laser (Tsunami, Spectra-Physics) set to a center wavelength of 760 nm. The laser intensity was modulated by using a Pockels cell (model 350–50 KDP*, Conoptics, Danbury, CT) and focused onto the specimen by a $\times$60/0.9 numerical aperture water immersion objective (Olympus). FRAP recordings were performed in the point-scan mode of the Fluoview system (sampling frequency 500 kHz, 2-ms binning). The laser intensity was set to a monitoring intensity of 4–10 mW (measured at the exit of the objective). After 0.3 s, a bleach pulse (6 ms, 35–65 mW) was applied, and the recovery of the fluorescence monitored for 1.5 s. After recording the fluorescence signal, the specimen background, laser intensity, and system background were recorded by using the same intensity protocol by defocusing, deflecting the (attenuated) laser beam directly toward the photomultiplier, and complete blockade of the laser beam, respectively. FRAP recordings were performed between 30 and 120 min after the whole-cell configuration was established.

Data analysis was performed with custom-written routines in IGOR PRO 5.0 (WaveMetrics, Lake Oswego, OR). The fluorescence data were corrected for the specimen background, and the laser intensity data were corrected for the system background. The fluorescence was subsequently divided by the square of the laser intensity (26) and normalized to the baseline fluorescence. The fluorescence recovery was fitted with an exponential function of the form

$$F(t) = 1 - f_i - f_m e^{-t/\tau} \quad [1]$$

were f_i and f_m are the fractions of total CB* that were immobilized and mobile, respectively, and were bleached (27); τ is the time constant of recovery. The sum of f_m and f_i is the bleach depth; the percentage of total immobilized CB is $100 \times f_i$/bleach depth. Following our previously described formalism (25), apparent diffusion coefficients (D) from FRAP experiments in spines were calculated as

$$D = \frac{\bar{l}\bar{V}}{\bar{\tilde{\tau}}\,\pi\,\overline{r^2}}, \quad [2]$$

where $\bar{l}$ is the mean length of spine necks, $\bar{V}$ is the mean effective (i.e., corrected for the endoplasmic reticulum) volume of spine heads, $\bar{\tilde{\tau}}$ is the mean of the median (among cells) FRAP time constants, and $\overline{r^2}$ is the expectation of the mean effective radius of spine necks squared (morphological values taken/calculated from ref. 28). The time constant of the relief of immobilization (τ_{slow}) was obtained from long-lasting (8–10 s) intermittent FRAP recordings that were fitted with a double-exponential function of the form

$$F(t) = 1 - f_i e^{-t/\tau_{slow}} - f_m e^{-t/\tau}. \quad [3]$$

For analyzing the influence of synaptic activity on immobilization of CB afferent climbing fibers (CFs) were stimulated repetitively (15 stimuli given at 1 or 20 Hz) with a glass pipette placed in the granule cell layer. The FRAP recordings were started jointly with the 13th CF stimulus. Unless stated otherwise, data are expressed as mean and SEM. The significance of differences was tested with a nested ANOVA (SIGMASTAT 3.10, Systat, Evanston, IL) with cells nested within treatments and repeated measurements taken on the same cell treated as replicates (no systematic effects of the order of measurement were observed).

Results

CB Is Immobilized in Spines and Dendrites but Not in Axons of PNs. We used two-photon FRAP (for review, see ref. 29) to quantify the mobility of CB* in PNs. Dialysis of PNs with CB* (200 μM) for at least 30 min via a somatic patch pipette homogenously labeled the entire neuron, allowing FRAP experiments in dendrites, spines, and axons (Fig. 1). FRAP in spines was characterized by an exponential but incomplete recovery after the bleach pulse (Fig. 1*B*). The time constant of recovery (τ) relates to diffusion of CB* between spines and dendrites (see below and ref. 25), whereas the incomplete return to baseline ("offset") relates to immobilization of a fraction of the spineous CB* (27, 29, 30). On average 19 $\pm$ 4% (n = 49, nine cells, eight animals) of the spineous CB* was immobilized on the time scale of the FRAP recordings.

The offset was not caused by technical problems such as bleaching or phototoxic damage because in FRAP experiments performed with dye-labeled 40-kDa dextran (500 μM) the fluorescence fully returned to baseline (Fig. 1*C*). Furthermore, in our previous FRAP analysis of the calcium-binding protein PV, performed under identical conditions, no offset was observed (25).

The partial immobilization of CB* was also observed in dendrites of PNs (Fig. 1*D*). On average, 28 $\pm$ 3% (n = 58, 13 cells, nine animals) of the dendritic CB* was immobilized, a value that was not significantly different from the immobilization occurring in spines. In contrast, FRAP recordings in axons showed a complete return to baseline (Fig. 1*E*, n = 13, three cells, three animals). These data indicate that immobilization of CB is specific to cellular compartments and that the binding partner is either immobile itself or of considerable size.

IMPase Immobilizes CB. Linse and coworkers (7) reported that CB is a constitutive (i.e., Ca^{2+}-independent) activator of IMPase *in vitro*. They also identified the putative CB-binding domain of IMPase-1 (residues 55–66, ISSIKEKYPSHS, IMP-P hereafter). We hypothesized that the immobilization of CB* occurring in spines and dendrites is caused by binding of CB* to IMPase and that the IMP-P could be used to compete with the CB*/IMPase interaction. Indeed, codialysis of CB* and the small, mobile IMP-P (400 μM) considerably reduced the immobilization of CB* (Fig. 2). In spines the immobilized fraction dropped from 19% to 4% (SEM 2%, n = 55, 11 cells, nine animals), and in dendrites it dropped from 28% to 8% (SEM 2%, n = 55, 10 cells, eight animals). For both compartments this change was highly significant ($P \leq 0.001$).

To assure that the effect of the IMP-P was specific, FRAP recordings were performed with a scrambled peptide that had,

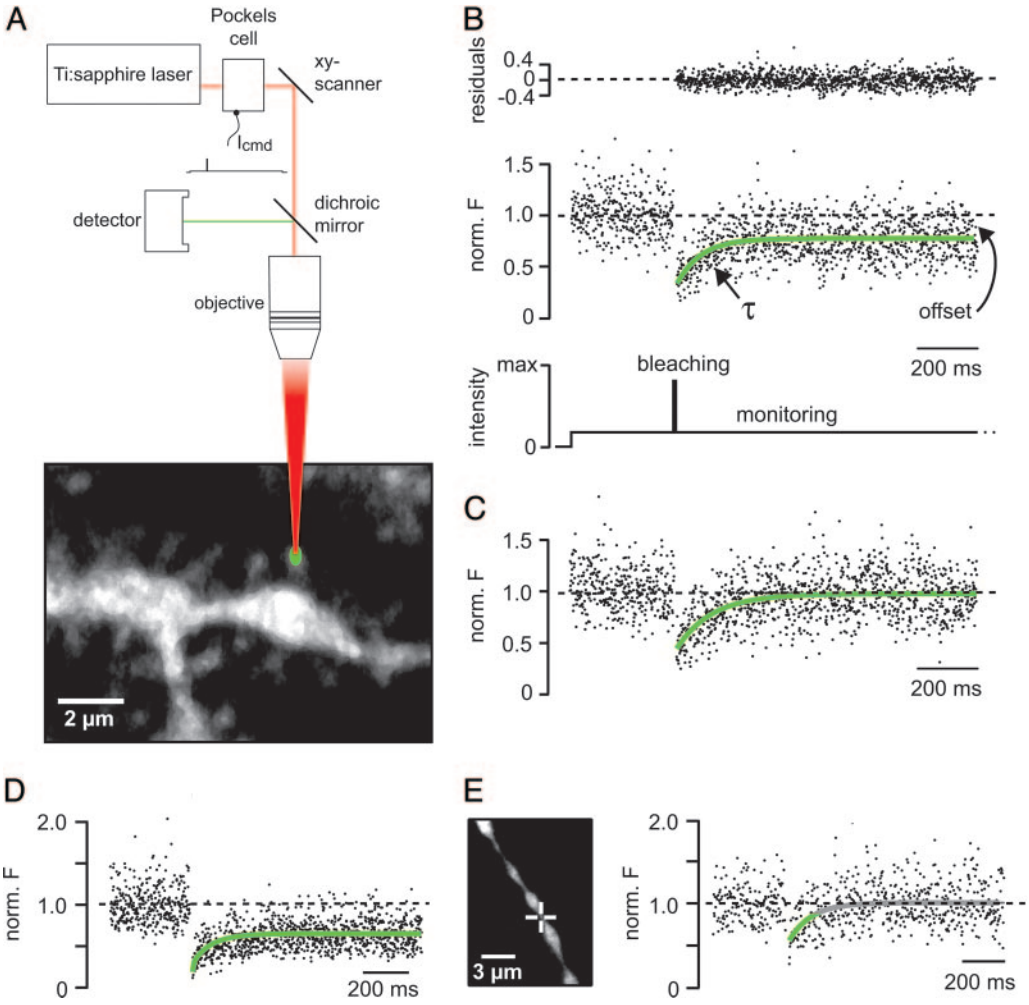

Fig. 1. CB* is partly immobilized in spines and dendrites but not in axons of cerebellar PNs. (*A*) Experimental set-up for FRAP recordings. Mode-locked laser light was intensity-modulated (I_{cmd}) by a Pockels cell and scanned with a custom-modified laser scanning microscope. The image shows spiny dendrites of a PN loaded with 200 μM CB* via a somatic patch pipette. For FRAP recordings the laser beam was focused on a single point of interest. (*B*) FRAP recording from the spine illustrated in *A*. The recovery (*Middle*) could be described by a single exponential function (green line; $\tau = 81$ ms) with an offset that indicates that 31% of CB* was immobilized in the spine. Shown are the residuals for the fit (*Top*) and the laser intensity (*Bottom*), respectively. (*C*) FRAP recording from a spine labeled with 40-kDa fluorescein dextran. Note the complete return to baseline. (*D* and *E*) FRAP of CB* in a dendritic (*D*) and an axonal (*E*) compartment of a PN. Note the presence and absence, respectively, of the offset.

in randomized sequence (SIKHPSKISEYS), the same amino acid composition as the IMP-P. Codialysis of the scrambled peptide (400 μM) did not affect the immobilization of CB* (Fig. 2*C*; immobilized fraction 27 ± 2% in dendrites ($n = 49$, 10 cells, seven animals) and 17 ± 2% in spines ($n = 17$, four cells, three animals). Thus, consistent with previous findings (7) the CB/IMP-P interaction appears to be specific. The decreased CB* immobilization is than readily explained by competition of the exogenous mobile peptide with the endogenous immobile IMPase protein.

The solubility of the IMP-P limited its final concentration in the pipette solution to ≈400 μM. Given the 1:1 (or 2:2; ref. 7) stoichometry of the CB/IMPase interaction, we used IMP-P in excess to CB* (pipette concentration of 200 μM). The fact that we could not completely mobilize CB* may be due to the lower affinity of CB for the peptide compared with that of the intact protein (7).

We next asked whether the CB*/IMPase interaction is modulated by synaptic activity. We choose the glutamatergic CF as the test input because it reliably evokes suprathreshold depolarizations, large Ca^{2+} signals (4), and probably substantial pH shifts (31) in PN dendrites. Hypothesizing that the CB/IMPase interaction may be affected by one or more of these postsynaptic responses (9), we performed FRAP recordings during ongoing CF stimulation. These recordings revealed a frequency-dependent increase of CB's immobilization to 38 ± 2% ($n = 24$, five cells, three animals) at 1 Hz and 47 ± 3% ($n = 43$, five cells, three animals) at 20 Hz; the latter value being significantly larger than the control ($P \leq 0.001$, Fig. 2*D*). Thus, the CB/IMPase interaction is regulated by synaptic activity *in situ*.

CB* Selectively Interacts with Immobilized IMPase. IMPase forms homodimers with a subunit molecular mass of 29 kDa (32) and exists in both a cytosolic and a membrane-bound form (33). The data presented so far indicate that the latter or an unidentified, otherwise fixed fraction of IMPase immobilizes CB. We addressed the question of whether cytosolic IMPase also interacts with CB by quantifying the diffusional mobility of CB*. For this purpose we analyzed FRAP time constants (τ) in spines (Fig. 1*B*), which relate to diffusional exchange between the spine and its parent dendrite and allow the calculation of the apparent diffusion coefficient (D) of CB* (25).

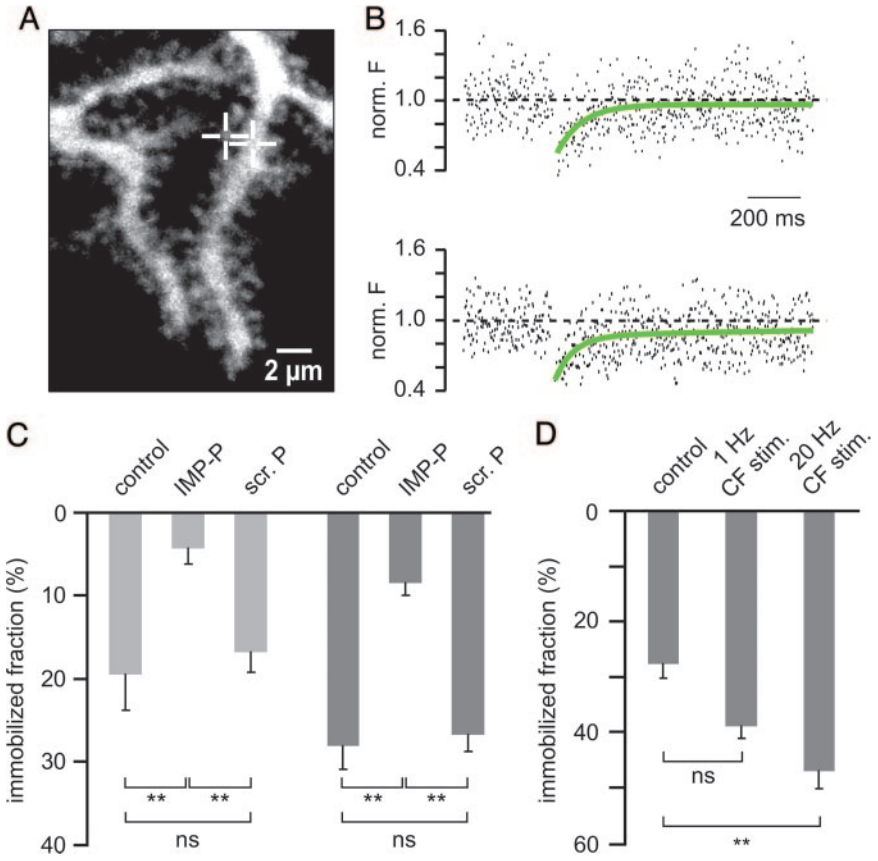

Fig. 2. CB* is immobilized by IMPase. (*A*) Image of spiny dendrites codialyzed with CB* and IMP-P, a synthetic peptide identical to the putative CB binding site of IMPase-1 (7). (*B*) FRAP recordings from the spine (*Upper*) and the parent dendrite (*Lower*) marked by crosshairs in *A*. Note the almost complete return to baseline. (*C*) Average immobilization of CB* in spines (*Left*) and dendrites (*Right*) under control conditions and in the presence of IMP-P or the scrambled control peptide (scr. P). (*D*) Immobilization of CB* in dendrites during ongoing synaptic stimulation (CF stim.). **, $P \leq 0.001$; ns, not significant.

Quantification of D values requires that τ values be independent of the bleach depth (26). The underlying formalism (Eq. **2**) predicts that τ values show a distribution skewed toward larger values (25). Both conditions were met in our recordings (Fig. 3 *A* and *B*). For individual cells as well as between cells there was only a moderate scatter of τ values (Fig. 3*C*). The average τ was 107 ms (SE of medians 9 ms, $n = 49$, nine cells, eight animals), a value that corresponds to a D_{CB*} of 20 ± 2 $\mu m^2/s$ (Eq. **2**).

In all FRAP recordings the time course of recovery was well described by a single exponential function (Fig. 1*B*), consistent with a single recovering species. However, this molecular species could have been either free CB*, CB* bound to mobile IMPase monomers, or CB* bound to IMPase dimers. As a further complication, the fluorescence recovery may have been influenced by binding and unbinding of CB* to/from immobile IMPase (29).

The Stokes–Einstein relation predicts (for spheroid molecules in aqueous solution) that diffusion coefficients are proportional to the inverse of the cubic root of the molecular weight of the diffusing species, i.e., $D \approx M^{-1/3}$. Assuming that CB* does not bind to cytosolic IMPase, its molecular mass would amount to ≈29 kDa. Comparing the measured D_{CB*} with our previously published diffusion coefficients of fluorescein dextrans and PV (25), we find that CB* diffuses slower than expected (Fig. 3*D*). This finding could indicate that CB forms heteromers with cytosolic IMPase and/or that interaction with membrane-bound IMPase slows down the diffusional exchange. However, in the presence of the IMP-P, which interferes with the CB/IMPase interaction, no acceleration of diffusion was observed. In contrast, D_{CB*} was slightly (but not significantly) reduced to 17 $\mu m^2/s$ ± 4 $\mu m^2/s$ ($n = 55$, 11 cells, nine animals, Fig. 3*D*), as expected if free CB* (29 kDa) interacts solely with IMP-P (1.4 kDa). Thus, as reported for PV (25), protein mobility in the dendritic microenvironment does not simply follow the Stokes–Einstein relation but seems to be determined by the tertiary structure of the proteins. Furthermore, either CB* does not interact with mobile, cytosolic IMPase or the latter is present only in minute amounts in spines and dendrites of PNs.

IMPase Immobilizes CB* on the Time Scale of Seconds. In a final set of experiments we analyzed the off-rate (k_{off}) of the CB/IMPase interaction, a central parameter for understanding the temporal dynamics of the interacting Ca^{2+} and inositol signaling cascades (34). The relief of immobilization was analyzed in long-lasting (8–10 s) FRAP recordings with intermittent illumination (to reduce the possibility of phototoxic damage). These recordings (Fig. 4) revealed that the immobilized fraction of CB* recovered with a time constant (τ_{slow}) of 13 s (10–16 s interquartile range, $n = 10$ spines, five cells, five animals). Given the large difference between τ_{slow} and the fast time constant of the fluorescence recovery (τ, Fig. 3), the slow phase of the fluorescence recovery is dominated by the reaction between CB* and IMPase (29, 35). Thus, k_{off} equals the inverse of τ_{slow}, i.e., ≈0.08 s^{-1}. From the K_D value of the CB/IMPase binding determined *in vitro* (0.9 μM, ref. 7), k_{on} can be estimated to be ≈9 × 10^4 $M^{-1}{\cdot}s^{-1}$.

Discussion

Two-photon FRAP allowed us to characterize *in situ* the interaction of two key molecules of distinct but coupled second

NEUROSCIENCE

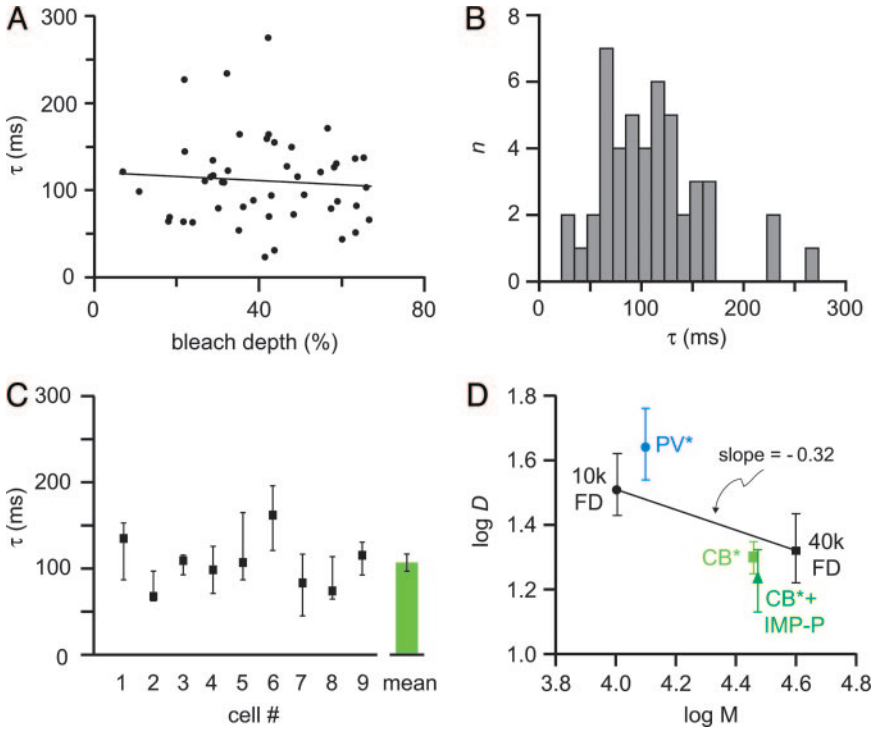

Fig. 3. Diffusional mobility of CB*. (*A*) Plot of FRAP time constants vs. bleach depth ($n = 49$ spine recordings, $r = -0,07$, solid line). (*B*) Distribution of τ values. (*C*) Variability of τ values within (median and interquartile range) and between cells (mean ± SE of medians). (*D*) Double-logarithmic plot of the derived apparent diffusion coefficients (*D*) of CB* in the absence (light green) and the presence (dark green) of IMP-P plotted against their molecular masses. The IMP-P was assumed to form (1:1) dimers with CB*. Published *D* values of 10- and 40-kDa fluorescein dextran (FD) and dye-labeled PV (PV*) are also shown (25). The line represents a linear fit to the FD data.

messenger cascades: CB and IMPase. CB is a relatively fast and high-capacity Ca^{2+} buffer that effectively shapes the waveform of intracellular Ca^{2+} signals (3, 4, 6). IMPase, on the other hand, regulates the breakdown and recycling of inositol messengers (19) that are linked to Ca^{2+} release from internal stores (22). Whereas previous *in vitro* data indicated that IMPase activity is increased by CB (7), we show that this interaction also occurs *in situ*, lasts for several seconds, is restricted to specific neuronal compartments, and is modulated by synaptic activity.

Little is known about the cellular distribution of IMPase. Our data indicate that IMPase is essentially immobile, e.g., targeted to membranes, and/or incorporated into large multimeric protein complexes in dendrites and spines but not in axons of PNs. Cytosolic, mobile IMPase is either not present at significant levels or does not bind CB. Given the importance of IP_3-mediated Ca^{2+} signaling for synaptic integration and plasticity in PNs (36–38), the CB/IMPase interaction is strategically placed at the site of metabotropic signaling.

The synaptically induced strengthening of the CB/IMPase interaction suggests that CB acts as a sensor that regulates the degradation of inositol messengers in an activity-dependent manner. It is tempting to speculate about the functional role of the CB/IMPase interaction for synaptic signaling. High-frequency synaptic activity is often associated with IP_3-mediated Ca^{2+} transients in PNs (36–38). Whereas these Ca^{2+} transients will be effectively buffered by CB (4), the activity-dependent

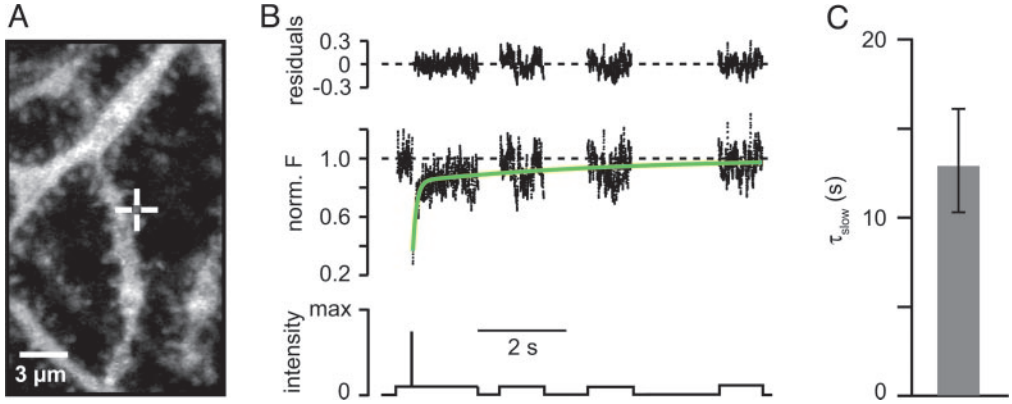

Fig. 4. Slow unbinding of CB* from IMPase. (*A*) CB*-labeled spiny dendrites. (*B*) Long-lasting, intermittent FRAP recording in the spine marked in *A*. The recovery could be described by the sum of two exponential functions (green line). The slow time constant (τ_{slow}) was 4.7 s. (*C*) Average τ_{slow} values (median ± interquartile range) from 10 spines from five cells.

targeting of CB to IMPase (this study) and the CB-dependent activation of IMPase (7) will accelerate the breakdown/recycling of IP_3 and, finally, allow the cell to maintain its responsiveness to inositol messengers. Thus, a long-lasting disturbance of the CB/IMPase interaction may substantial deteriorate IP_3-mediated signaling. Support for this hypothesis comes from a recent study of Barski *et al.* (5) who stated that IP_3-mediated Ca^{2+} signaling (quantified by using Ca^{2+} indicator dyes) is not altered in PNs of CB knockout mice compared with the WT. However, considering that CB strongly reduces the amplitude of dendritic Ca^{2+} signals (3, 4), Barski *et al.*'s data indicate that, indeed, loss of CB results in strongly diminished IP_3-mediated Ca^{2+} release.

Albeit rather indirect, evidence for a link between CB and IMPase is provided by the functional deficits associated with these two molecules. Whereas loss of CB is associated with cerebellar ataxia in mice (3, 5), IMPase is linked to the pathogenesis/treatment of bipolar disease in humans (see, for review, ref. 21). Interestingly, postmortem studies of bipolar disease patients revealed a loss of CB immunoreactivity in the CNS (39). Furthermore, a form of inherited bipolar disease is associated with ataxia (40), and cerebellar ataxia is a common sign of Li^+ overdosing in the treatment of bipolar disease (41–43).

In addition to the effect on inositol signaling, the CB/IMPase interaction may directly affect Ca^{2+} buffering by CB. The immobilization of CB will affect the spatiotemporal spread of Ca^{2+} signals in spines and dendrites, and binding to IMPase may directly affect the Ca^{2+} affinity of CB, similar to the increased Ca^{2+} affinity of calmodulin after binding of target peptides (44). Clearly, further experimentation will be necessary to dissect the functional consequences of the CB/IMPase interaction on the densely interwoven IP_3 and Ca^{2+} signaling network in central neurons.

We thank G. Betghe for technical help, D. Gitler and M. Heckmann for comments on the manuscript, T. Kawecki for comments on the statistics, G. Dale (Morphochem, Basel) for the purification of recombinant CB, and S. Rothemund (Interdisziplinäres Zentrum für Klinische Forschung, Leipzig, Germany) for the peptide synthesis. This work was supported by Deutsche Forschungsgemeinschaft Grant Ei 342/2, the Bundesministerium für Forschung und Bildung, and Swiss National Science Foundation Grants 3100-063448.00/1 and 3100A0-100400 (to B.S.).

1. Baimbridge, K. G., Celio, M. R. & Rogers, J. H. (1992) *Trends Neurosci.* **15,** 303–308.
2. Nägerl, U. V., Novo, D., Mody, I. & Vergara, J. L. (2000) *Biophys. J.* **79,** 3009–3018.
3. Airaksinen, M. S., Eilers, J., Garaschuk, O., Thoenen, H., Konnerth, A. & Meyer, M. (1997) *Proc. Natl. Acad. Sci. USA* **94,** 1488–1493.
4. Schmidt, H., Stiefel, K., Racay, P., Schwaller, B. & Eilers, J. (2003) *J. Physiol. (London)* **551,** 13–32.
5. Barski, J. J., Hartmann, J., Rose, C. R., Hoebeek, F., Mörl, K., Noll-Hussong, M., De Zeeuw, C. I., Konnerth, A. & Meyer, M. (2003) *J. Neurosci.* **23,** 3469–3477.
6. Blatow, M., Caputi, A., Burnashev, N., Monyer, H. & Rozov, A. (2003) *Neuron* **38,** 79–88.
7. Berggård, T., Szczepankiewicz, O., Thulin, E. & Linse, S. (2002) *J. Biol. Chem.* **277,** 41954–41959.
8. Berggård, T., Miron, S., Önnerfjord, P., Thulin, E., Åkerfeldt, K. S., Enghild, J. J., Akke, M. & Linse, S. (2002) *J. Biol. Chem.* **277,** 16662–16672.
9. Berggård, T., Silow, M., Thulin, E. & Linse, S. (2000) *Biochemistry* **39,** 6864–6873.
10. Venters, R. A., Benson, L. M., Craig, T. A., Paul, K. H., Kordys, D. R., Thompson, R., Naylor, S., Kumar, R. & Cavanagh, J. (2003) *Anal. Biochem.* **317,** 59–66.
11. Lutz, W., Frank, E. M., Craig, T. A., Thompson, R., Venters, R. A., Kojetin, D., Cavanagh, J. & Kumar, R. (2003) *Biochem. Biophys. Res. Commun.* **303,** 1186–1192.
12. Morgan, D. W., Welton, A. F., Heick, A. E. & Christakos, S. (1986) *Biochem. Biophys. Res. Commun.* **138,** 547–553.
13. Bellido, T., Huening, M., Raval-Pandya, M., Manolagas, S. C. & Christakos, S. (2000) *J. Biol. Chem.* **275,** 26328–26332.
14. Reisner, P. D., Christakos, S. & Vanaman, T. C. (1992) *FEBS Lett.* **297,** 127–131.
15. Leathers, V. L. & Norman, A. W. (1993) *J. Cell. Biochem.* **52,** 243–252.
16. Hubbard, M. J. & McHugh, N. J. (1995) *FEBS Lett.* **374,** 333–337.
17. Winsky, L. & Kuźnicki, J. (1995) *J. Neurochem.* **65,** 381–388.
18. Belmaker, R. H. (2004) *N. Engl. J. Med.* **351,** 476–486.
19. Gee, N. S., Ragan, C. I., Watling, K. J., Aspley, S., Jackson, R. G., Reid, G. G., Gani, D. & Shute, J. K. (1988) *Biochem. J.* **249,** 883–889.
20. Yoshikawa, T., Turner, G., Esterling, L. E., Sanders, A. R. & Detera-Wadleigh, S. D. (1997) *Mol. Psychiatry* **2,** 393–397.
21. Atack, J. R. (1996) *Brain Res. Brain Res. Rev.* **22,** 183–190.
22. Berridge, M. J., Downes, C. P. & Hanley, M. R. (1982) *Biochem. J.* **206,** 587–595.
23. Williams, R. S. B., Cheng, L., Mudge, A. W. & Harwood, A. J. (2002) *Nature* **417,** 292–295.
24. Schwaller, B., Durussel, I., Jermann, D., Herrmann, B. & Cox, J. A. (1997) *J. Biol. Chem.* **272,** 29663–29671.
25. Schmidt, H., Brown, E. B., Schwaller, B. & Eilers, J. (2003) *Biophys. J.* **84,** 2599–2608.
26. Brown, E. B., Wu, E. S., Zipfel, W. & Webb, W. W. (1999) *Biophys. J.* **77,** 2837–2849.
27. Star, E. N., Kwiatkowski, D. J. & Murthy, V. N. (2002) *Nat. Neurosci.* **5,** 239–246.
28. Harris, K. M. & Stevens, J. K. (1988) *J. Neurosci.* **8,** 4455–4469.
29. Sprague, B. L., Pego, R. L., Stavreva, D. A. & McNally, J. G. (2004) *Biophys. J.* **86,** 3473–3495.
30. Luby-Phelps, K., Hori, M., Phelps, J. M. & Won, D. (1995) *J. Biol. Chem.* **270,** 21532–21538.
31. Willoughby, D. & Schwiening, C. J. (2002) *J. Physiol. (London)* **544,** 487–499.
32. Atack, J. R., Broughton, H. B. & Pollack, S. J. (1995) *FEBS Lett.* **361,** 1–7.
33. Vadnal, R. E., Parthasarathy, R., Parthasarathy, L., Ramesh, T. G. & Shyamaladevi, C. S. (1992) *Biochem. Int.* **26,** 935–941.
34. Bhalla, U. S. & Iyengar, R. (1999) *Science* **283,** 381–387.
35. Bulinski, J. C., Odde, D. J., Howell, B. J., Salmon, T. D. & Waterman-Storer, C. M. (2001) *J. Cell. Sci.* **114,** 3885–3897.
36. Finch, E. A. & Augustine, G. J. (1998) *Nature* **396,** 753–756.
37. Takechi, H., Eilers, J. & Konnerth, A. (1998) *Nature* **396,** 757–760.
38. Wang, S. S.-H., Denk, W. & Häusser, M. (2000) *Nat. Neurosci.* **3,** 1266–1273.
39. Reynolds, G. P., Abdul-Monim, Z., Neill, J. C. & Zhang, Z. J. (2004) *Neurotoxicol. Res.* **6,** 57–61.
40. Fernandez Piqueras, J., Santos, J., Visedo, G., Perez de Castro, I., Puertollano, R., Montejo, J., Ramo Tello, C. & Valle, J. (1995) *Am. J. Med. Genet.* **60,** 206–209.
41. Roy, M., Stip, E., Black, D. N., Lew, V. & Langlois, R. (1999) *Can. J. Psychiatry.* **44,** 671–679.
42. Ferbert, A. & Czernik, A. (1987) *Nervenarzt* **58,** 764–770.
43. Dembowski, C. & Rechlin, T. (2003) *Pharmacopsychiatry* **36,** 83–86.
44. Peersen, O. B., Madsen, T. S. & Falke, J. J. (1997) *Protein Sci.* **6,** 794–807.